Sandia National Laboratories

SAND2020-7801C

Noise and error reduction in particle based kinetic simulations

Z Fundamental Sciences Workshop 2020

E.G. Evstatiev[1], J.M. Finn[2], B.A. Shadwick[3], N. Hengartner[4]

[1]Sandia National Laboratory, Albuquerque, NM
[2]Tibbar Plasma Technologies, Los Alamos, NM
[3]University of Nebraska-Lincoln, Lincoln, NE
[4]Los Alamos National Laboratory, Los Alamos, NM

Sandia National Laboratories is a multimission laboratory managed and operated by National Technology & Engineering Solutions of Sandia, LLC, a wholly owned subsidiary of Honeywell International Inc., for the U.S. Department of Energy's National Nuclear Security Administration under contract DE-NA0003525.

Motivation

- Noise in particle based simulations is still an important issue
- Low level/amplitude physics may be difficult to simulate
- Coupling between time dependent fluid and particles in δf methods becomes problematic because of high levels of noise in the charge and current densities
- Noise becomes a worse problem in quasi-neutral plasmas
- Using the familiar scaling $1/\sqrt{N_p}$ to reduce noise quickly becomes computationally expensive/prohibitive
- No analytical method for noise and error estimation and control exists at present
- The total error in the estimated charge/current density is not just the variance (the $1/\sqrt{N_p}$ term) but has another, equally important but less familiar contribution, the *bias*

Scope of analysis

- This analysis is restricted to:
  - Periodic systems (on the interval [0,1])
  - Electrostatic (Vlasov-Poisson)
  - Charge-neutral plasmas
  - Mobile electrons and immobile ions
  - Constant and equal weight computational particles
  - Spatial analysis on uniform grid (non-Fourier models)
  - Noise and error in the charge density and electric field

Density estimation by finite number of particles

- Write the density distribution function as

$$f_e(x,v,t) = \sum_{\mu=1}^{N_p} q_\mu K(x-\xi_\mu)\delta(v-\dot{\xi}_\mu)$$

- Integrating we have at *any* spatial point, i.e., continuous x

$$\rho_e(x) = \sum_{\mu=1}^{N_p} q_\mu K(x-\xi_\mu)$$

- In our analysis, the *kernel* $K(x)$ is generally *not* the familiar PIC particle shape; it satisfies these conditions:

  - Normalized to unity,
  $$\int_0^1 dx\, K(x) = 1\,;$$
  - Symmetric, $K(x) = K(-x), \quad x \in [0,1]$;
  - Translationally invariant, $K(x,\xi) = K(x-\xi), \quad x,\xi \in [0,1]$;
  - Nonnegative, $K(x) \geq 0, \quad x \in [0,1]$;
  - Has compact support.

- The normalization to unity assures conservation of total charge in the system.

Fundamental kernel

- We separate the kernel *shape* from *width* by working with a *fundamental kernel* of support one ([-1/2, 1/2]):

$$K(x) = \frac{1}{h} K_f\left(\frac{x}{h}\right)$$

- The following table shows some examples that are used in the following:

Kernel	Definition
Boxcar (top-hat)	$K_{fB}(x) = \begin{cases} 1, \; \lvert x\rvert \le \frac{1}{2} \\ 0 \text{ otherwise}. \end{cases}$
Linear (tent)	$K_{fL}(x) = \begin{cases} 2\left(1 - 2\lvert x\rvert\right), \; \lvert x\rvert \le \frac{1}{2} \\ 0 \text{ otherwise}. \end{cases}$
Quadratic	$K_{fQ}(x) = 9 \begin{cases} \frac{1}{4} - 3x^2, \; \lvert x\rvert \le 1/6 \\ \frac{3}{2}\left(\frac{1}{2} - \lvert x\rvert\right)^2, \; 1/6 \le \lvert x\rvert \le 1/2 \\ 0 \text{ otherwise}. \end{cases}$
Trapezoidal	$K_{fT}(x) = \frac{3}{2} \begin{cases} 1, \; \lvert x\rvert \le 1/6 \\ 3\left(\frac{1}{2} - \lvert x\rvert\right), \; 1/6 \le \lvert x\rvert \le 1/2 \\ 0 \text{ otherwise}. \end{cases}$
Epanechnikov	$K_{fE}(x) = \begin{cases} \frac{3}{2}\left(1 - 4x^2\right), \; \lvert x\rvert \le \frac{1}{2} \\ 0 \text{ otherwise}, \end{cases}$

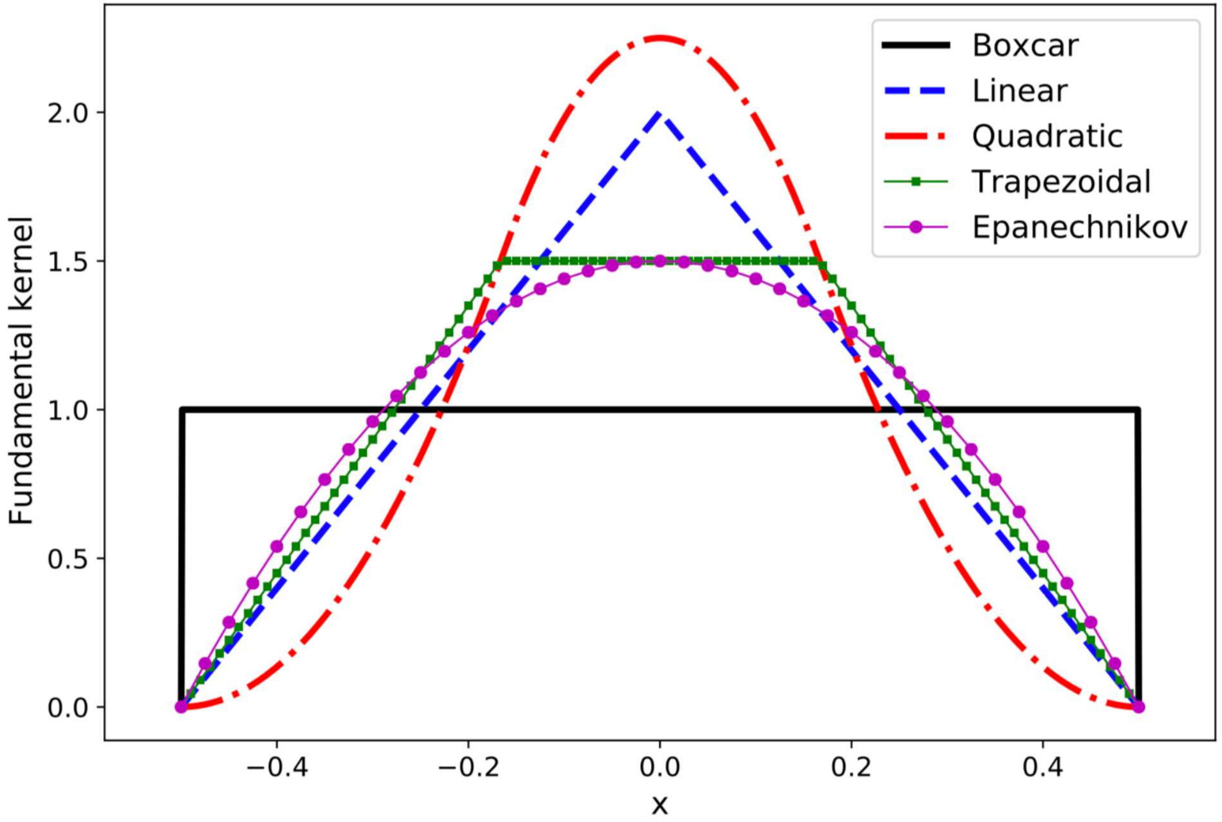

Statistical analysis in uniform density: variance

- We distinguish between *true* density, $\rho(x)$, and *estimated* density $\rho_e(x)$ (estimated via the finite number of computational particles).

- Using $\int_0^1 \rho(x) = 1$ and $\rho(x) \geq 0$ (also assuming $\int_0^1 \rho^{(i)}(x)dx = 1$), we can use $\rho(x)$ as a probability distribution and calculate ensemble averages for any $f(x)$ as $\langle f(x)\rangle = \int_0^1 dx\, f(x)\rho(x)$.

- Thus, the ensemble average of the estimated over the true density is

$$\langle \rho_e(x)\rangle = \left(\sum_{\mu} q_\mu\right)\int_0^1 K(x-\xi)\rho(\xi)d\xi = \rho(x) + \frac{h^2}{2}\rho''(x)\int_{-1/2}^{1/2} K_f(\eta)\eta^2 d\eta + \cdots .$$

- For uniform density $\rho(x) = 1$ (hence $\rho''(x) = 0$) and only the first term above remains. We have $\rho_e(x) = \langle \rho_e(x)\rangle + \tilde{\rho}_e(x) = 1 + \tilde{\rho}_e(x)$ and we can write the *variance* as

$$V(x) = \langle \tilde{\rho}_e(x)^2\rangle = \langle \rho_e(x)^2\rangle - 1 = V_d(x) + V_o(x) - 1 = V_d(x) - 1/N_p.$$

- Notice the *negative contribution* to the variance, which arise because of the *finite number of particles*

Statistical analysis in uniform density: covariance matrix

- The *covariance matrix* relates the density at two different points x and y and we calculate the density correlations as

$$C(x,y) = \langle \tilde{\rho}_e(x)\tilde{\rho}_e(y)\rangle = \langle \rho_e(x)\rho_e(y)\rangle - 1$$

- Detailed averaging calculations lead to

$$C(x,y) = C(x-y) = C_d(x-y) - \frac{1}{N_p}.$$

- Notice again the negative term, which is the same as the one for the variance. For the special case of a δ-function kernel $K(x)$ we obtain

$$C(x-y) = \frac{1}{N_p}\left[\delta(x-y) - 1\right].$$

- The covariance matrix satisfies the *general property* (easily verified on the special case above)

$$\int dy\, C(x,y) = \int dy\, C(x-y) = 0\,.$$

Statistical analysis of the electric field

- We use Gauss's law to compute the electric field

$$\frac{dE}{dx} = \rho^{(i)} - \rho_e = \rho_q \quad \text{with} \quad \int_0^1 dx\, E(x) = 0 \quad \text{(charge neutrality condition)}$$

- The general solution for any density distribution (notice independence on the initial point of integration) is:

$$E(x) = \int_0^x dz\, \rho_q(z) + \int_0^1 dx\, x\rho_q(x) \equiv E_1(x) + E_0$$

- The covariance matrix becomes (including variance, i.e., the diagonal terms) is given by:

$$C^E(x,y) = \int_0^1 zdz \int_0^1 wdwC(z,w) + \int_0^1 wdw \int_0^x C(w,z)dz + \int_0^1 zdz \int_0^y C(z,w)dw + \int_0^x dz \int_0^y dwC(z,w).$$

- For the special case of δ-function kernel this reduces to the *translationally invariant* form

$$C^E(x,y) = \frac{1}{2N_p}\left[-|x-y| + (x-y)^2 + \frac{1}{6}\right]$$

- The E-field correlations also satisfy the general property $\int dx\, C^E(x,y) = 0$

Statistical analysis of the electric field: Ornstein-Uhlenbeck bridge

- The electric field correlations for the δ-function case may be cast into the form

$$C^E(x,y) = \frac{1}{N_p}\left[\min(x,y) - xy + \frac{x(x-1)}{2} + \frac{y(y-1)}{2} + \frac{1}{12}\right]$$

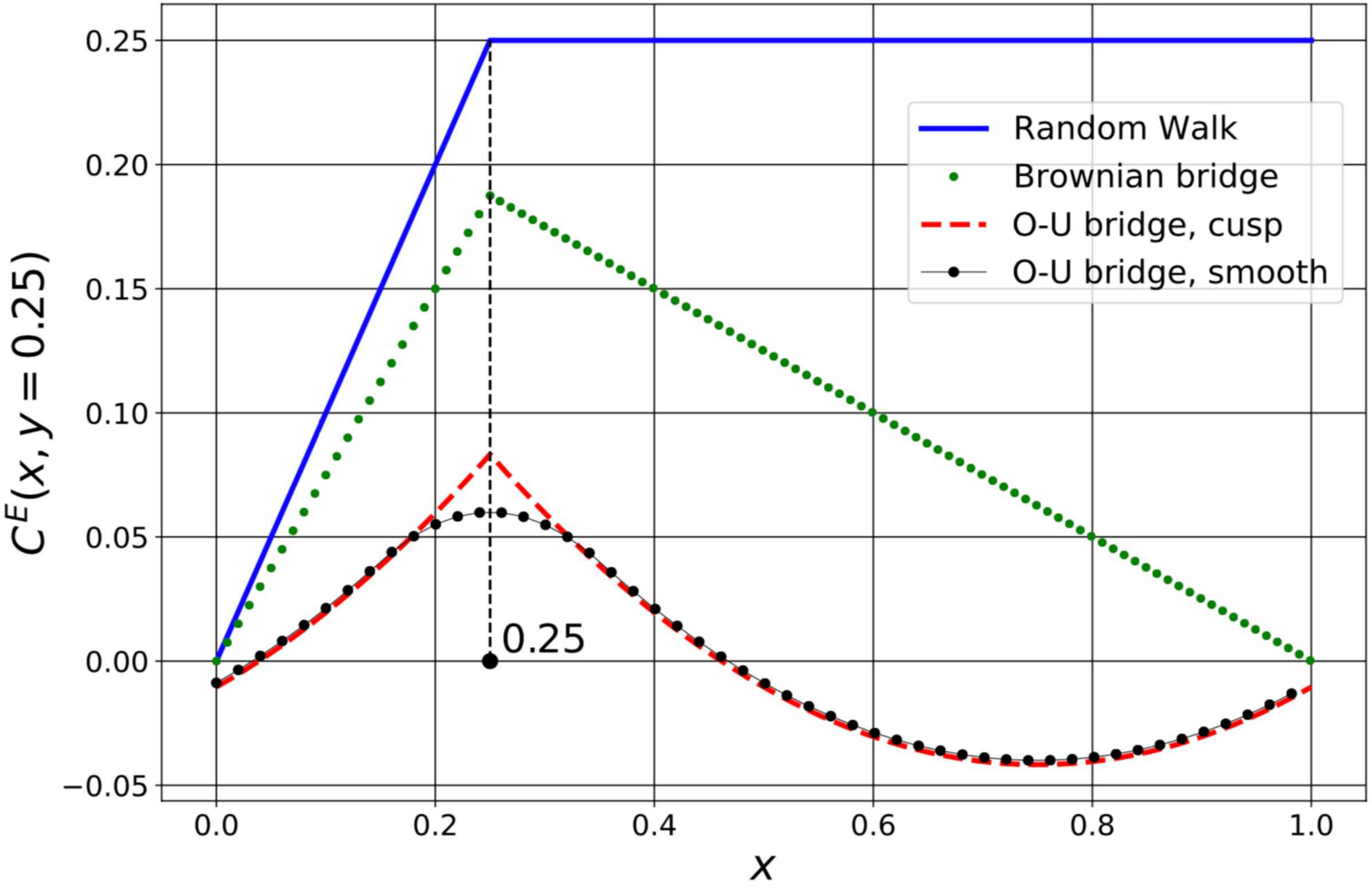

Statistical analysis in non-uniform density: bias-variance opt.

- Recall the general expansion

$$\langle \rho_e(x) \rangle = \rho(x) + \frac{h^2}{2}\rho''(x)\int_{-1/2}^{1/2} K_f(\eta)\eta^2 d\eta + \cdots .$$

- Now the second derivative is not zero, $\rho''(x) \neq 0$; the total error (squared) in estimating the density is

$$Q = \left\langle \left(\rho_e(x) - \rho(x)\right)^2 \right\rangle = V + B^2 = \frac{\rho(x)C_1}{N_p}\frac{1}{h} + \frac{\rho''(x)^2 C_2^2}{4}h^4$$

with *shape coefficients* $C_1 = \int_{-1/2}^{1/2} K_f(\zeta)^2 d\zeta\,, \qquad C_2 = \int_{-1/2}^{1/2} \zeta^2 K_f(\zeta) d\zeta$

- We can extremize the total error Q with respect to the kernel width h (*bias-variance optimization/trade-off*):

$$h = h_{\text{opt}} = \left(\frac{\rho(x)C_1}{N_p \rho''(x)^2 C_2^2}\right)^{1/5}, \qquad h = h_{\text{opt,av}} = \left(\frac{C_1}{N_p\left(\int \rho''(x)^2 dx\right) C_2^2}\right)^{1/5},$$

$$Q_{\text{min}} = \frac{5}{4}\left(\frac{\rho(x)|\rho''(x)|^{1/2} C_1 C_2^{1/2}}{N_p}\right)^{4/5} \qquad Q_{\text{min,av}} = \frac{5}{4}\left(\frac{\left(\int dx\,|\rho''(x)|^2\right)^{1/4} C_1 C_2^{1/2}}{N_p}\right)^{4/5}$$

(mean square error) (mean integrated square error)

Examples: bias-variance optimization curves

- The following table gives the values of the coefficients C_1 and C_2 and sketches of the averaged BVO curves for $\int_0^1 dx\, \rho(x) = \int_0^1 dx\, \rho''(x) = 1$.

Kernel	C_1	C_2	$\left(C_1 C_2^{1/2}\right)^{4/5}$	$(C_1/C_2^2)^{1/5}$	$(C_1 C_2^3)^{2/5}$
Boxcar	1	1/12	0.370	2.70	0.0507
Linear (tent)	4/3	1/24	0.353	3.78	0.0248
Quadratic	33/20	1/36	0.356	4.63	0.0166
Trapezoidal	5/4	5/108	0.350	3.57	0.0274
Epanechnikov	6/5	1/20	0.349	3.44	0.0295

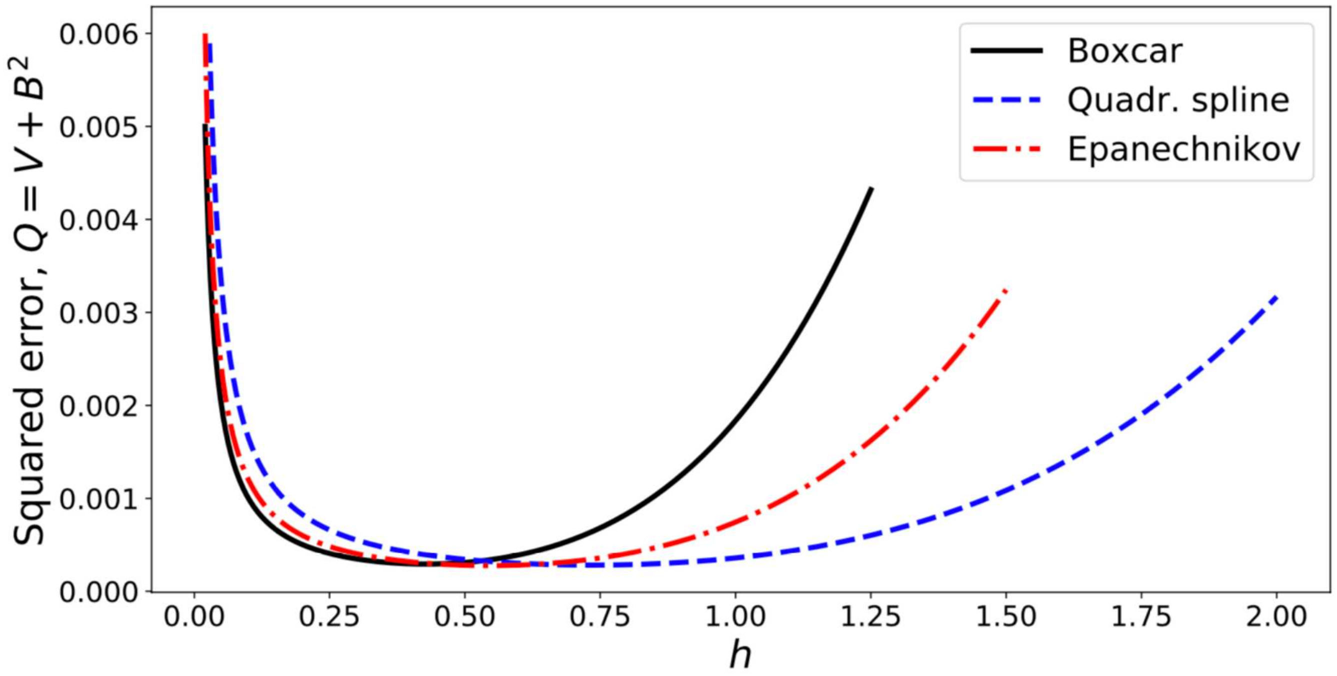

Statistical analysis in non-uniform density: scaling arguments

- Some conclusions that can be drawn from the above results:
  - The *variance (V)*, is a *finite number* of particles effect
  - The *bias (B),* is a *finite size* of particles effect
  - The *bias-variance optimization* process leads to a *minimum of the total error* in estimated density
  - The minimum of the total error minimum error $Q_{\min}$ scales as $N_p^{-4/5}$, which is *weaker* than the variance scaling N_p^{-1} (i.e., the usual noise scaling as $1/\sqrt{N_p}$)
  - The balance between variance and bias (squared) occurs when

$$\frac{1}{\rho(x)N_p h} \sim \frac{\rho''(x)^2}{\rho(x)^2} h^4 \sim \left(\frac{h}{l}\right)^4$$

where the typical *gradient scale length* is given by $l = \sqrt{\rho(x)/|\rho''(x)|}$

  - The quantity on the left is interpreted as the number of particles within a length h. We may say that the variance term dominates if we have too few particles within l while the bias term dominates when the kernel width h increases too much relative to l
  - The optimal width of the kernel scales as $h_{\text{opt}} \sim (\cdots)^{1/5}$, i.e., weakly depends on the total number of particles, etc.
  - The width of the minimum curve scales as $Q''(h_{\text{opt}}) \sim (\cdots)^{2/5}$, therefore we expect a relatively broad minimum of the curve $Q(h)$, as seen in the figure

Grid discretization: kernels vs. particle shapes and the sum rule

- The continuous variables formulas are "absolute" in the sense that they do not require or suppose the existence of a grid
- The discretization of the formulas is straightforward; the type and accuracy of discretization are dictated by choice and need to resolve the simulated physics
- One important connection that must be made is between the Lagrangian particles and the Eulerian grid. This is done with a *charge deposition rule* provided by a *particle shape*. The extact conservation of charge, after being deposited *on the grid* is a basic requirement in particle methods. The following *sum rule* assures the latter:

$$\sum_{i=1}^{N_g} \Delta\, S(x_i - \xi) = 1$$

- The conventional particle shapes (splines) have two unnecessary restrictive properties:
  - Width always being an integer number of cells
  - Width always related to their smoothness
- These properties can also become computationally inefficient when the BVO width is larger than 4 cells, i.e., require higher than 4^{th} order splines
- The distinction between kernels $K(x)$ and particle shapes $S(x)$ is at the heart of relaxing the above restrictions; notice that S(x) satisfies all conditions that K(x) does plus the extra condition of the sum rule. Therefore, S(x) can always be use as a kernel for the density estimate but K(x) in general cannot be used as a particle shape.

Obtaining particle shapes by convolution

- The following convolution between a (known) particle shape (or finite element) and an arbitrary kernel always produces a particle shape (satisfying all kernel properties plus the sum rule):

$$S(x) = \int dy\, K(y) S_0(x-y)\,.$$

- Examples:

Particle shape	Definition
Boxcar (NGP)	$S_B(x) = \frac{1}{\Delta}\begin{cases} 1, \; \lvert\frac{x}{\Delta}\rvert \le \frac{1}{2} \\ 0 \text{ otherwise}\,. \end{cases}$
Linear spline	$S_L(x) = \frac{1}{\Delta}\begin{cases} 1 - \lvert\frac{x}{\Delta}\rvert, \; \lvert\frac{x}{\Delta}\rvert \le 1 \\ 0 \text{ otherwise}\,. \end{cases}$
Quadratic spline	$S_Q(x) = \frac{1}{\Delta}\begin{cases} \frac{3}{4} - \left(\frac{x}{\Delta}\right)^2, \; \lvert\frac{x}{\Delta}\rvert \le 1/2 \\ \frac{1}{2}\left(\frac{3}{2} - \lvert\frac{x}{\Delta}\rvert\right)^2, \; 1/2 \le \lvert\frac{x}{\Delta}\rvert \le 3/2 \\ 0 \text{ otherwise}\,. \end{cases}$
Trapezoidal	$S_T(x) = \frac{1}{\Delta}\begin{cases} \frac{1}{2}, \; \lvert\frac{x}{\Delta}\rvert \le 1/2 \\ \frac{1}{2}\left(\frac{3}{2} - \lvert\frac{x}{\Delta}\rvert\right), \; 1/2 \le \lvert\frac{x}{\Delta}\rvert \le 3/2 \\ 0 \text{ otherwise}\,, \end{cases}$

- Obtaining shapes by convolution is only sufficient but not necessary, i.e., other methods may lead to obtaining particle shapes (which by definition satisfy the sum rule).

Particle shapes of non-integer cell width

- It is not necessary to use particles of integer width, as the following example shows the convolution between a boxcar shape with a boxcar kernel of width $0 \leq \delta \leq \Delta$:

$$S_{\Delta+\delta}(x) = \int dy\, K_\delta(y) S_B(x-y)$$

$$= \frac{1}{\Delta} \begin{cases} 1, & 0 \leq |x| \leq \frac{\Delta-\delta}{2} \\ \frac{1}{\delta}\frac{\Delta+\delta}{2} - \left|\frac{x}{\delta}\right|, & \frac{\Delta-\delta}{2} \leq |x| \leq \frac{\Delta+\delta}{2} \\ 0, & \text{otherwise}\,. \end{cases}$$

where $K_\delta(x) = \frac{1}{\delta} \begin{cases} 1, & \left|\frac{x}{\delta}\right| \leq \frac{1}{2} \\ 0 & \text{otherwise}\,. \end{cases}$

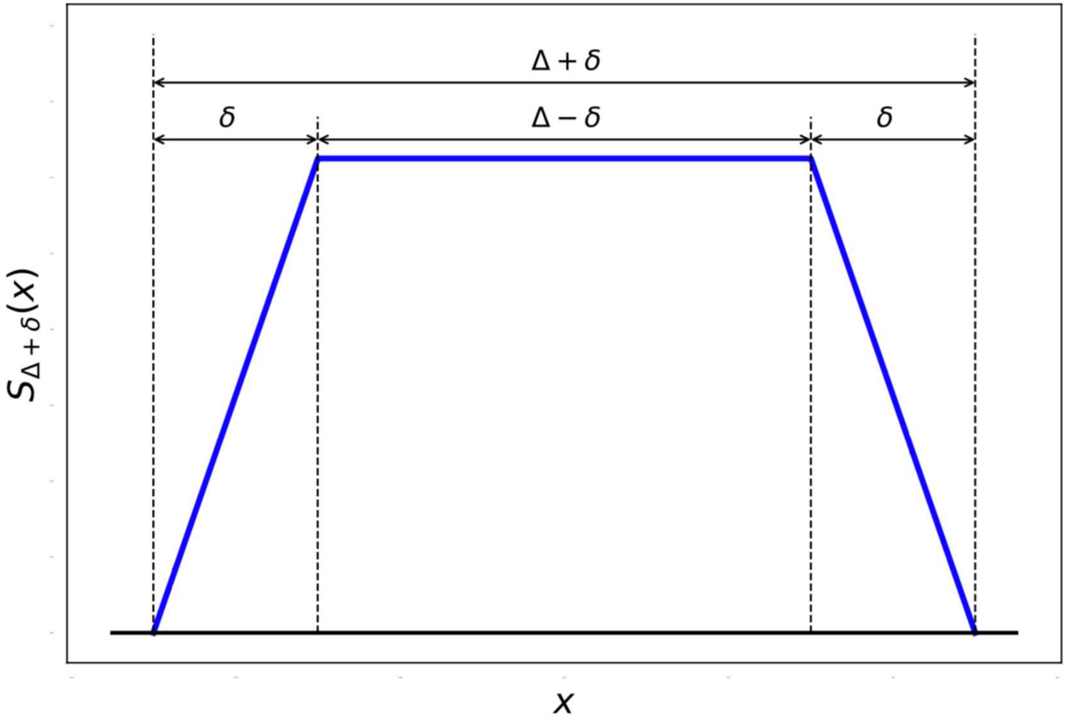

Charge deposition rule	Range
$S_{i-1}(\xi) = 0$ $S_i(\xi) = \frac{1}{\Delta}$ $S_{i+1}(\xi) = 0$	$0 \leq \lvert\xi - x_i\rvert \leq \frac{\Delta-\delta}{2}$
$S_{i-1}(\xi) = \frac{1}{\Delta\delta}\left[-\frac{\Delta-\delta}{2} - (\xi - x_i)\right]$ $S_i(\xi) = \frac{1}{\Delta\delta}\left[\frac{\Delta+\delta}{2} + (\xi - x_i)\right]$ $S_{i+1}(\xi) = 0$	$-\frac{\Delta}{2} \leq \xi - x_i \leq -\frac{\Delta-\delta}{2}$
$S_{i-1}(\xi) = 0$ $S_i(\xi) = \frac{1}{\Delta\delta}\left[\frac{\Delta+\delta}{2} - (\xi - x_i)\right]$ $S_{i+1}(\xi) = \frac{1}{\Delta\delta}\left[-\frac{\Delta-\delta}{2} + (\xi - x_i)\right]$	$\frac{\Delta-\delta}{2} \leq \xi - x_i \leq \frac{\Delta}{2}$

Examples of uniform density correlations on a grid

- Density discretization (at cell centers) gives the following correlation formulas for familiar particle shapes

$$C_{i+1/2,j+1/2} = \frac{1}{N_{ppc}}\delta_{ij} - \frac{1}{N_p}. \qquad \text{(Boxcar (NGP))}$$

$$C_{i+1/2,j+1/2} = \begin{cases} \frac{1}{N_p}\left[\Delta \int S(\xi)^2 d\xi - 1\right] = \frac{1}{N_p}\left[\frac{2}{3\Delta} - 1\right] = \frac{2}{3N_{ppc}} - \frac{1}{N_p} & (j = i), \\ \frac{1}{N_p}\left[\Delta \int S(\xi - 1)S(\xi) d\xi - 1\right] = \frac{1}{6N_{ppc}} - \frac{1}{N_p} & (j = i \pm 1), \\ -\frac{1}{N_p} & \text{otherwise.} \end{cases} \qquad \text{(Linear)}$$

$$C_{i+1/2,j+1/2} = \begin{cases} \frac{11}{20N_{ppc}} - \frac{1}{N_p} & (j = i) \\ \frac{13}{60N_{ppc}} - \frac{1}{N_p} & (j = i \pm 1) \\ \frac{1}{120N_{ppc}} - \frac{1}{N_p} & (j = i \pm 2) \\ -\frac{1}{N_p} & \text{otherwise.} \end{cases} \qquad \text{(Quadratic)}$$

- The sum rule is essential to have the discrete property $\sum_j C_{i+1/2,j+1/2} = 0$ (analogous to $\int dy\, C(x,y) = 0$)

Numerical results in uniform density: correlations on a grid

- We rewrite the correlations for the *linear charge deposition* in normalized form:

$$\widetilde{C}_{i+\frac{1}{2},i+\frac{1}{2}} \equiv C_{i+\frac{1}{2},i+\frac{1}{2}} \times N_{ppc} = \frac{2}{3} - \Delta\,,$$
$$\widetilde{C}_{i+\frac{1}{2},i+\frac{1}{2}\pm 1} \equiv C_{i+\frac{1}{2},i+\frac{1}{2}\pm 1} \times N_{ppc} = \frac{1}{6} - \Delta$$

- The table shows numerical simulations on a *fixed grid* with $N_g = 25$ and varying particle numbers and samples:

N_p	M	$\widetilde{C}_{i+\frac{1}{2},i+\frac{1}{2}}$		$\widetilde{C}_{i+\frac{1}{2},i+\frac{1}{2}\pm 1}$	
		theoretical	numerical	theoretical	numerical
250	2.5×10^6	0.6266...	0.6269	0.1266...	0.1267
2500	2.5×10^5		0.6256		0.1251
25,000	2.5×10^4		0.6208		0.1252

- The sample number that yields satisfactory comparison with theory is about 10^6; this number is used in all following simulations

Numerical results in non-uniform density: setup

- As a true density we use:

$$\rho(x) = 1 + a\cos(2\pi m x)\,, \qquad x \in [0,1]$$

- For all simulations we use $a = 0.5$ and $m = 2$. For most simulations we use $N_p = 10^4$.

- The scaling transform $K(x) = K_f(x/h)/h$ is implemented by using the same particle shape but changing the grid spacing. For example, three-cell-wide particles have a width $h = 3\Delta = 3/15 = 0.2$ (with $\Delta = 1/N_g$) and number of grid points $N_g = 15$; for $N_g = 30$ we have width $h = 3/30 = 0.1$, etc.

- We also use the Epanechnikov kernel (scaled to 3Δ) for comparison since it provides the lowest minimum error among all other kernel shapes (however, it does *not* satisfy the sum rule, i.e., it is not a particle shape):

$$K_E(x) = \frac{1}{\Delta}\begin{cases} \frac{1}{2}\left(1 - \frac{4}{9}\left(\frac{x}{\Delta}\right)^2\right), & \left|\frac{x}{\Delta}\right| \le \frac{3}{2} \\ 0 & \text{otherwise}\,. \end{cases}$$

Numerical results in non-uniform density: scaling argument

- In non-uniform density, we are interested in the local error, i.e., at a fixed spatial location; we take $x = 1/2$
- At $x = 1/2$ we have $\rho(1/2) = 3/2$ and $\rho''(1/2) = -8\pi^2$. The gradient scale length is $l = \sqrt{1.5/8\pi^2} \simeq 0.138$. Looking into a range $N_g \in [16, 48]$ for a kernel of width $h = \Delta$, we plot the bias and variance curves

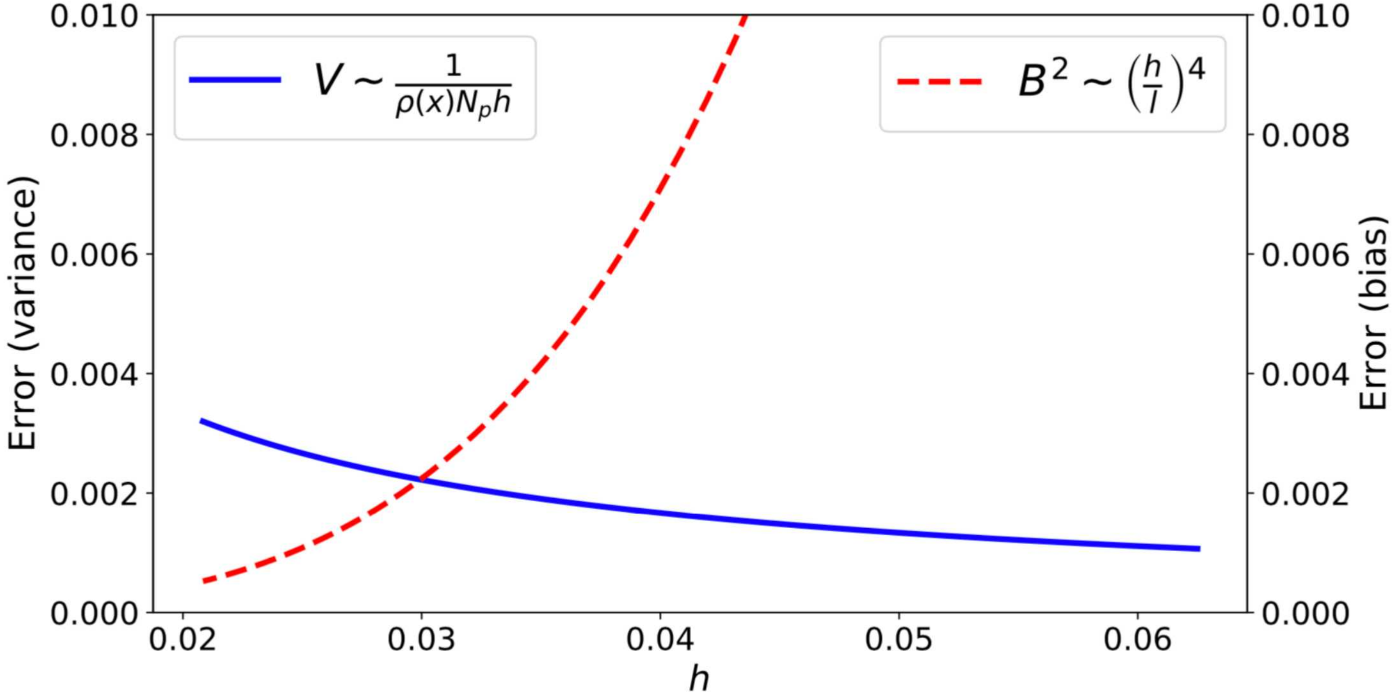

- We see that the curves cross and we expect to have a minimum of the total error in the range $N_g \in [16, 48]$

Numerical results in non-uniform density: quantitative study

- At $x = 1/2$ and $N_g \in [16, 48]$ we compare numerically $Q(h)$ for all four kernels. We observe a minimum for all curves with excellent agreement with theory

Shape	$Q_{\min}$ theoretical	$Q_{\min}$ numerical	h_{opt} theoretical	h_{opt} numerical
Boxcar	0.00232	0.00206	0.0810	0.0833
Quadr. spline	0.00223	0.00198	0.139	0.136
Trapezoidal	0.00219	0.00194	0.107	0.107
Epanechnikov	0.00219	0.00194	0.103	0.107

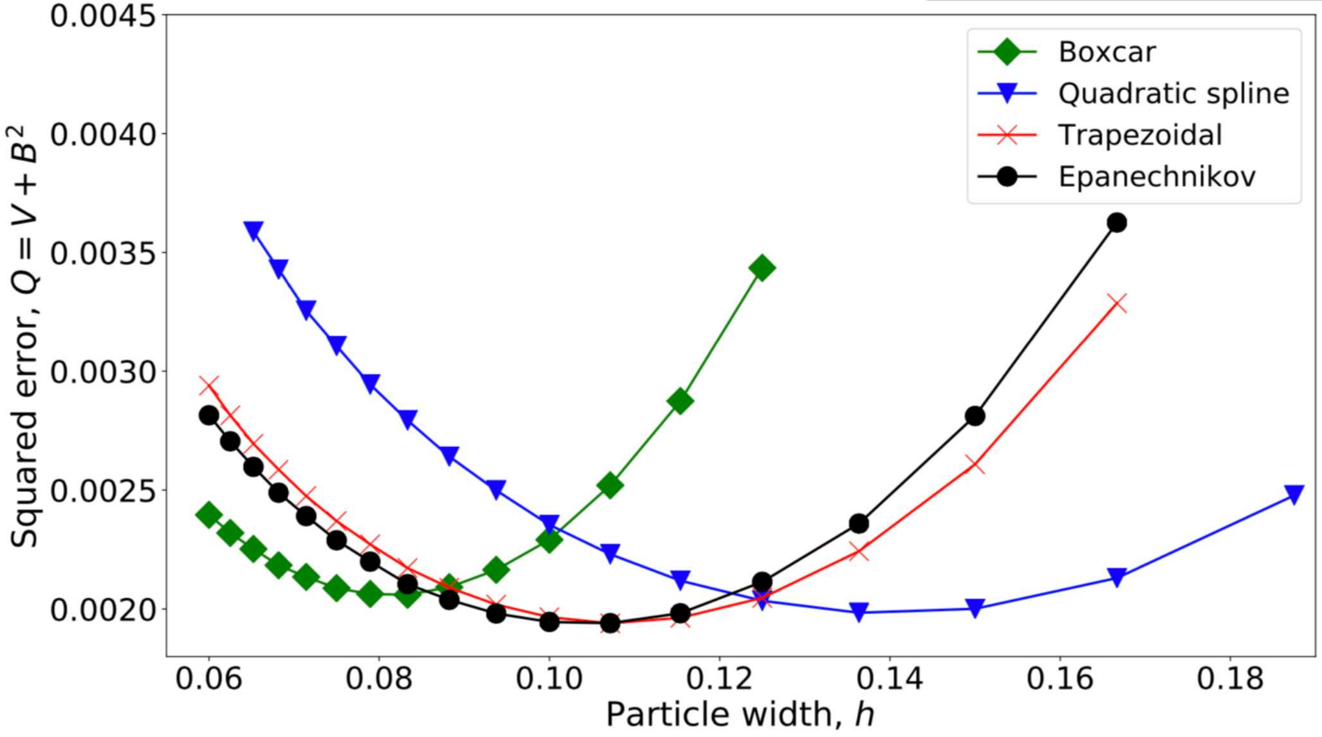

Numerical results in non-uniform density: fractional cell width shape

- The fractional width particle shape can also be used to operate near the minimum of $Q(h)$.
- With this shape, no change in the charge deposition scheme is necessary. However, changing its width $\Delta + \delta$ is *not* a pure scaling but a parametric shape and width transform (therefore the previous formulas do not directly apply).
- The results for two fixed grids are shown below at $x = 1/2$; the discontinuity is expected and is where the grid changes size $N_g = 16 \to 8$

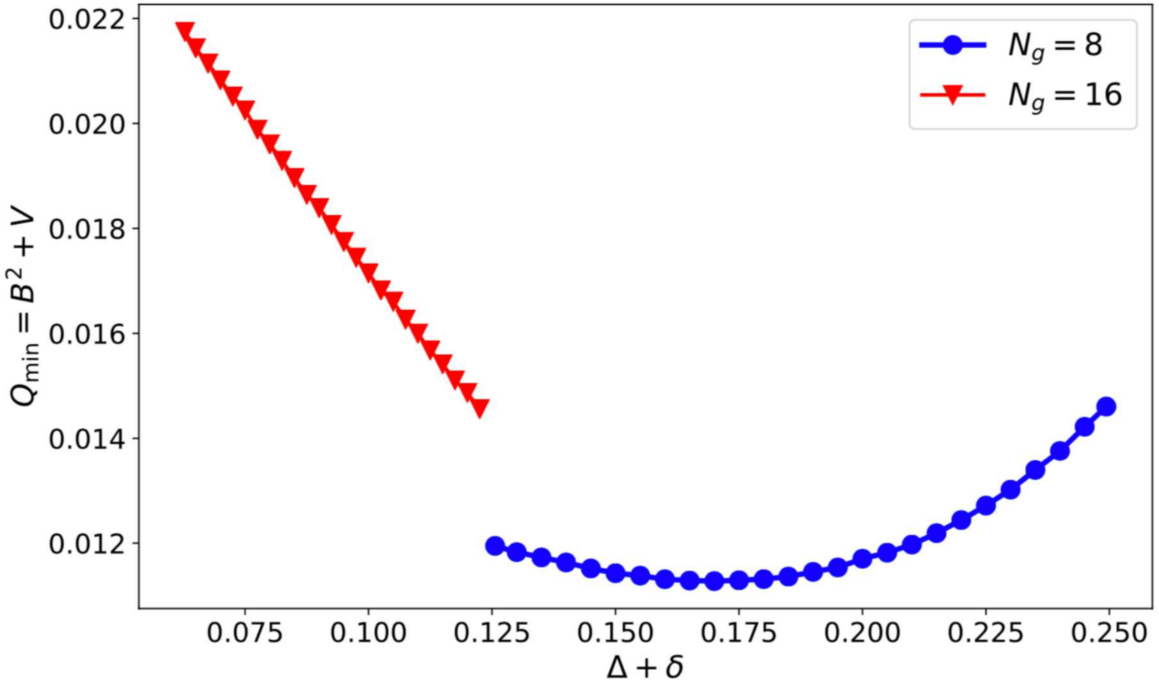

Conclusions and future work

- Conclusions:
  - The noise and error have been analyzed in uniform and non-uniform density distributions
  - In uniform charge density the finite number of particles lead to a constant small but non-negligible negative contribution to all covariance matrix elements (diagonal and off-diagonal)
  - The negative contributions lead to correlations described by the Ornstein-Uhlenbeck bridge
  - In non-uniform density there is an additional error contribution from the finite size of computational particles, the bias
  - The process of bias-variance optimization leads to an optimal kernel/particle width that minimizes the total error
  - The scaling of the minimum error with number of particles is weaker than the usual variance scaling
  - On a discrete grid, particles of arbitrary (uncoupled) width and smoothness may be constructed by the convolution of a kernel and a particle shape (or finite element)
  - Numerical results and theory agree very well

- Future work:
  - Analyze the remaining two steps: (i) errors in the E-field leading to errors in the particle force; and (ii) errors in the particle trajectories leading to errors in the charge density, i.e., *closing the loop*
  - Generalization to electromagnetic models, where the current density must be analyzed; generalization to 2D and 3D